Pentacene thin films on ferromagnetic oxide: Growth mechanism and spintronic devices

P. Graziosi, A. Riminucci, M. Prezioso, C. Newby, D. Brunel, I. Bergenti, D. Pullini, D. Busquets-Mataix, M. Ghidini, and V. A. Dediu

Articles you may be interested in

Hanle effect missing in a prototypical organic spintronic device
Appl. Phys. Lett. **102**, 092407 (2013); 10.1063/1.4794408

Manipulating spin injection into organic materials through interface engineering
Appl. Phys. Lett. **101**, 022416 (2012); 10.1063/1.4737008

Planar-type spin valves based on low-molecular-weight organic materials with La 0.67 Sr 0.33 Mn O 3 electrodes
Appl. Phys. Lett. **92**, 153304 (2008); 10.1063/1.2905288

Room temperature organic spintronics
J. Appl. Phys. **103**, 07F306 (2008); 10.1063/1.2829245

Application of regioregular polythiophene in spintronic devices: Effect of interface
Appl. Phys. Lett. **89**, 122114 (2006); 10.1063/1.2356463

Pentacene thin films on ferromagnetic oxide: Growth mechanism and spintronic devices

P. Graziosi,[1,2] A. Riminucci,[1] M. Prezioso,[1,a)] C. Newby,[1,b)] D. Brunel,[1,c)] I. Bergenti,[1]
D. Pullini,[3] D. Busquets-Mataix,[2,4] M. Ghidini,[5,6] and V. A. Dediu[1]

[1]CNR - ISMN, Consiglio Nazionale delle Ricerche - Istituto per lo Studio dei Materiali Nanostrutturati,
v. Gobetti 101, 40129 Bologna, Italy
[2]Instituto de Tecnología de Materiales, Universitat Politécnica de Valencia, Camino de Vera s/n, 46022,
Valencia, Spain
[3]Centro Ricerche Fiat, 10043 Orbassano (TO), Italy
[4]Departamento de Ingeniería Mecánica y de Materiales, Universitat Politécnica de Valencia,
Camino de Vera s/n, 46022, Valencia, Spain
[5]Department of Physics, University of Parma, v. le G.P. Usberti 7/A, 43100 Parma, Italy
[6]Department of Materials Science, University of Cambridge, Cambridge CB3 0FS, United Kingdom

We investigated the growth mechanism of pentacene thin films on $La_{0.7}Sr_{0.3}MnO_3$. A diffusion limited, thermally activated growth was found. Pentacene molecules formed flat islands that were a few microns in size and whose growth during deposition showed a strong anisotropy. We extracted a nucleation energy of 0.65 ± 0.05 eV and a diffusion barrier energy of 0.7 ± 0.2 eV. We also estimated a critical nucleus size of three molecules. We show that vertical pentacene-based spintronic devices with $La_{0.7}Sr_{0.3}MnO_3$ and Co electrodes demonstrated magnetoresistive effects up to room temperature. We also propose a route for pentacene-based spintronic devices improvement. © 2014 AIP Publishing LLC. [http://dx.doi.org/10.1063/1.4890328]

Spintronics is a branch of electronics, where the information is carried by the spin degree of freedom of the electron. Thanks to their small spin-orbit coupling,[1] organic semiconductors (OSCs) are promising candidates as spin transporting media in spintronics.[2] Since the first successful demonstration of spin transport through organic semiconductors,[3] organic spintronics have been the object of increasing interest and gave rise to conceptually new devices.[4,5]

Electrically driven spintronic devices are usually fabricated by separating two spin polarized electrodes by a charge and spin conducting non-magnetic layer. The detected effect consists in a resistance modification caused by the variation of the relative spin polarization of the electrodes. The parallel and the antiparallel configurations have two distinct resistances, resulting in the so called spin valve effect.

Aromatic hydrocarbon semiconductors have the best electrical properties among OSCs.[6] In particularly, pentacene, which has the relatively high mobility of 5 $cm^2/(Vs)$,[7] is one of the most used in organic electronics.[6] Despite this, its investigation in spintronics is limited to a very few cases. Spintronic effects at 5.3 K were reported for planar devices with $La_{0.7}Sr_{0.3}MnO_3$ (LSMO) electrodes and a pentacene spacer[8] (a spin diffusion length exceeding 200 nm was proposed in this paper) and in vertical devices comprising a Fe top electrode and a composite Co:TiO_2 bottom electrode separated by a 100 nm thick pentacene spacer.[9] On the other hand, no magnetoresistance (MR) effects were detected in pentacene-based devices fabricated without oxide

electrodes,[10] unless oxidizing the pentacene layer in plasma oxygen.[11] Thus, available data point to the crucial role of oxides, and in particular of LSMO, as electrode materials for pentacene-based spintronics; indeed, LSMO is by far the most used spin polarized electrode in organic spintronics.[12]

In this report, we present a spin valve device based on pentacene as OSC spacer and on LSMO and Co as ferromagnetic electrodes, operating up to room temperature (RT). In order to pave the way for improved spintronic devices, we also investigated the pentacene growth on top of LSMO thin film surfaces.

LSMO films were grown on $SrTiO_3(100)$ (STO) with a homemade channel spark ablation set-up.[13] Prior to pentacene deposition, LSMO films were annealed *in situ* in ultra high vacuum (UHV) in order to clean the surface and to restore the surface properties.[14] Pentacene films with thicknesses between 3 nm and 100 nm were subsequently deposited at a base pressure of 10^{-8} mbar with a homemade organic molecular beam deposition system at a fixed rate of 0.003 nm/s. Atomic force microscopy (AFM) was carried out with a Nanoscope III microscope, and the analysis was performed with the Gwyddion software package.[15]

Figure 1 presents the resistance of a LSMO/pentacene/Al_2O_3/Co spin valve as function of the in plane applied magnetic field **H**, the pentacene thickness is 100 and 300 nm; area junction, defined by shadow masking, is 1 mm^2. The measurement was carried out with a Keithley 236 in the four probe configuration, with an applied bias of -0.1 V (grounded Co) at 100 K and at room temperature. Similar structures, with Alq_3 as OSC spacer, were widely studied.[4,12,16,17] The Al oxide buffer layer was deposited by channel spark ablation of an alumina target in oxygen environment at room temperature[18] in order to preserve the

a)Present address: University of California, Santa Barbara, Electrical & Computer Engineering Harold Frank Hall, Santa Barbara, CA 93106-9560.
b)Present address: Intel, Portland, Oregon Area.
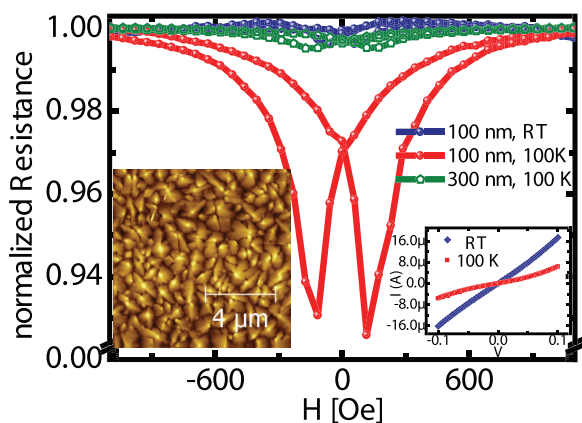c)Present address: Ecole Polytechnique, Route de Saclay, Palaiseau, France.

FIG. 1. Magnetoresistance of a LSMO/pentacene(100 nm and 300 nm)/Al$_2$O$_3$(2.5 nm)/Co spin valve measured at 100 K and at RT with a −0.1 V applied bias (grounded Co). The left hand side inset shows a $10 \times 10 \ \mu m^2$ AFM image of the pentacene film covered by 2 nm of Al$_2$O$_3$; the z scale is 45 nm. The right hand side inset shows the IV curves at room temperature and 100 K for the 100 nm case; their behaviour with temperature is semiconducting-like.
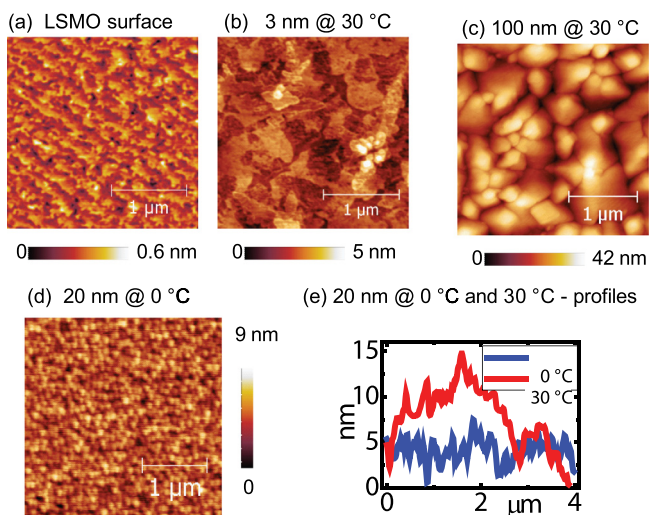

FIG. 2. (a) AFM morphology of the LSMO surface. (b) and (c) AFM micrographs showing the morphology of 3 nm and 100 nm thick pentacene films, respectively, deposited at 30 °C on LSMO; (d) AFM micrograph of 20 nm thick pentacene film deposited at 0 °C on LSMO; (e) peak-to-valley comparison of 20 nm films deposited at 0 °C and 30 °C.

properties of both pentacene and Co, as done in Alq$_3$ based devices.[12,18] After each step, the vacuum was broken for a couple of minutes to change the shadow masks. The pentacene films were deposited at room temperature in order to make the results comparable to those from the previous report on LSMO/pentacene spin valves[8] and to those obtained with other OSCs.[4,8,10,17,19] An AFM micrograph of the pentacene surface after the Al$_2$O$_3$ deposition is reported in the left inset in Figure 1.

The figure of merit of the spin valve device is its MR = (R$_{AP}$ − R$_P$)/R$_P$, where R$_P$ and R$_{AP}$ are the device resistance in the parallel and antiparallel state, respectively. The device with 100 nm nominal pentacene layer shows a MR of −7% at 100 K and −0.4% at RT, which is in line with the room temperature MR of Alq$_3$-based spin valves.[16] In analogy with Alq$_3$ devices, the negative sign of the MR can be tentatively attributed to the interface energy levels alignment.[16,20] Since the nominal thickness of the pentacene film is 100 nm and the peak to valley height difference is 45 nm, conductive paths of different lengths are present, and hence, the effective spin transport length is much smaller than the nominal thickness of the pentacene spacer. Nevertheless, the Co and LSMO electrodes are not shorted: the current-voltage characteristic (right inset in Figure 1) as a function of temperature shows a semiconducting behaviour. The device with 300 nm pentacene nominal thickness shows, at 100 K, a MR about −0.3% and no MR at RT, a similar trend was observed in devices based on transport in Alq$_3$.[16] Considering also that the sign of the MR of LSMO/Al$_2$O$_3$/Co junctions is the opposite of the one we detect,[21] we rule out pinholes effects.

Having demonstrated the suitability of pentacene as a spin transporting medium in combination with LSMO, it is necessary to study the pentacene film growth mechanism on LSMO in order to establish the relevant parameters for further device improvement.

The LSMO surface (Figure 2(a)) showed 200 nm wide terraces with a roughness smaller than a unit cell: the root mean square roughness R$_{rms}$ was about 0.13 ± 0.02 nm.

Figure 2(b) shows an AFM micrograph of a pentacene film with a nominal thickness of 3 nm deposited on LSMO at 30 °C. The first monolayer forms a wetting layer with a morphology which is radically different from the one of the LSMO. The subsequent molecules grow on this pentacene wetting layer and form three dimensional islands with an anisotropic shape, presumably due to the elongated shape of the pentacene molecules; anisotropic growth of pentacene on SiO$_2$ is well known.[22]

Apart from the wetting layer, growth is anisotropic at all stages: Figure 2(c) shows the surface of a 100 nm nominal thickness pentacene film deposited at room temperature on LSMO. The islands in the 100 nm thick film are smaller and with a higher density than the islands at earlier stages of growth. This effect is the signature of a growth that is limited by the Ehrlich–Schwoebel (ES) barrier, which prevents the diffusing molecules from going over the edge of a terrace, thus confining them on a step.[23] ES barrier-controlled growth leads to a three dimensional growth which results in a roughening of the film.[24] This roughening is called "rapid" because it grows with the film thickness faster than in the random deposition model (RD), where molecules attach where they arrive, without diffusion.[25] In general, it is valid that $R_{rms} \sim t^{\beta}$, where t is the nominal film thickness and β is the growth exponent; in the RD model $\beta = 0.5$.[25] Rapid roughening occurs when $\beta > 0.5$, and is known for pentacene and other organic molecules deposited on SiO$_2$,[25,26] for pentacene deposited on LSMO we obtain $\beta = 0.6 \pm 0.1$.

Figure 2(d) reports the morphology of a 20 nm thick pentacene film deposited on LSMO at a measured temperature of 0 °C. A higher nucleation rate is observed but not a higher roughness: $R_{rms} \sim 1.3$ nm and peak-to-valley roughness is about 10 nm. Figure 2(e) compare the peak-to-valley roughness of two 20 nm thick films deposited at RT and 0 °C – the AFM morphology of 20 nm pentacene films deposited on LSMO is comprehensively described in Ref. 27. The rapid roughening seems to be suppressed and the pentacene film looks more compact: low temperature deposition

could be a promising approach for devices with vertical transport.

More information comes from the scaling exponent α (static roughness exponent), obtained from the height-height correlation function g: $g_{(t_x,t_y)} = \frac{1}{N}\int\int \left(z_{(x,y)} - z_{(x+t_x,y+t_y)}\right)^2 dxdy$, where z is the height of the point having (x,y) coordinates and N is the total number of points. For $t_x, t_y \ll \xi$, $g \sim R^{2\alpha}$, where ξ is the surface correlation length and $R = \sqrt{t_x^2 + t_y^2}$.[26,28] For pentacene films grown on LSMO between 30 °C and 60 °C, α does not depend on the substrate temperature but increases with the film thickness from 0.67 ± 0.05 at 3 nm to 0.80 ± 0.03 at 100 nm. These values are indicative of a diffusion limited growth,[29] a picture which will be assumed in what follows.

Figure 3 reports the topography of 3 nm thick pentacene films deposited at different temperatures. The size of the pentacene islands increases with deposition temperature, as does the interisland distance. Figure 3(f) shows that the inter-island region in a sample deposited at 75 °C is very similar to bare LSMO. While the LSMO surface looks completely covered when a 3 nm pentacene film is deposited at 30 °C, the coverage is not complete and the wetting layer disappears when pentacene is deposited above 40–45 °C. The thermal energy at 40–45 °C is sufficient to overcome the interaction of pentacene molecules with the substrate, while on SiO$_2$ a temperature of at least 80 °C is needed.[24] The flat morphology over a large area shown in Figures 3(b)–3(e) has been previously observed only on SiO$_2$, and only when the growth was assisted by a supersonic gas flow that gave molecules a high kinetic energy and hence a high surface diffusivity.[30] The analysis of the effective coverage, obtained by measuring the volume of the islands,[15] shows that it decreases from 75% at a substrate temperature of 45 °C to 55% at 75 °C: at this temperature desorption could start to play a significant role.[31] All together, data in Figure 3 demonstrate that the molecule-substrate interaction is weak when pentacene grows on LSMO.

The energy landscape was studied quantitatively by means of the stable island density model,[32] according to which the island surface density is given by $n \approx \exp(E_N/k_B T)$, where E_N is a global nucleation energy. When islands grow by capturing both the molecules landing on them directly and those that diffused from other sites on the substrate, $E_N = \frac{E_{i*} + i^* \cdot E_D}{(i^*+2)}$ or $\frac{E_{i*} + i^* \cdot E_D}{(i^*+2.5)}$ depending on whether the growth bi-dimensional or three-dimensional, respectively.[32] i^* is the critical molecules number, i.e., the minimum number of molecules needed to form a stable nucleus, E_D is the barrier to molecules diffusion on the substrate and E_{i*} is the formation energy for a stable nucleus. E_{i*} is expressed as $E_{i*} = \sum_{m=2}^{i^*} E_m$, where E_m is the formation energy of a nucleus of m molecules.

In order to apply this nucleation model, we excluded the data from deposition at 30 °C and at 75 °C; in the former case because of the wetting layer which looked to disappears at T $\geq$ 40 °C, in the latter because desorption started to play a significant role. From the Arrhenius plot in Figure 4(a), we extracted $E_N = 0.65 \pm 0.05$ eV for $40 \leq$ T ≤ 60 °C. This energy scale is confirmed by ultra-violet photoemission spectroscopy measurements of a 0.4 eV energy dipole between pentacene and LSMO,[27] which is low if compared to the 1 eV found for pentacene deposited on Co.[33,34] The E_N value for pentacene on LSMO can be compared with the nucleation energy found for pentacene grown on SiO$_2$ over the same temperature range: $E_N = 0.78 \pm 0.05$ eV was found for a growth rate of 0.007 nm/s,[35] which is similar to the one used in the present experiment. At higher growth rates (0.03 nm/s) $\sum_{m=2}^{i^*} E_m + i^* E_D = 1.13 \pm 0.04$ eV and $i^* = 3$ were reported,[36] hence $E_N = 0.23 \pm 0.01$ eV. Considering that E_N varies with the growth rate,[31] the value we extracted for pentacene on LSMO is compatible with the one for SiO$_2$ substrates (Figure 4(b)), assuming that at lower rates E_N levels off rather than diverging.[35,37] Pentacene nucleation and growth on LSMO are much closer to those on SiO$_2$ than those on Co.[34]

The diffusion mechanism was analysed in order to disentangle the contributions of diffusion and nucleation in E_N. The surface diffusion length is defined as $x_s = \sqrt{D_s \tau}$, where D_s is the diffusion coefficient and τ is the residence time, i.e., the time the molecule moves on the substrate before attaching or desorbing. x_s is estimated as the mean distance between the centre of the islands.[38] Since $D_s = a^2 \omega e^{(E_D/k_B T)}$ and $\tau = \omega^{-1} e^{(E_a/k_B T)}$, where a and ω are the pentacene molecules' jump distance and jump rate, respectively, the diffusion distance is $x_s \approx e^{((E_D + E_a)/k_B T)}$. Due to the above consideration about the diffusion limited character of the growth, we can approximate x_s with $x_s \sim e^{(E_D/2k_B T)}$, which gives $E_D = 0.7 \pm 0.2$ eV for T $\geq$ 40 °C (Figure 4(c)).

Based on the values of E_N and E_D, we discuss i^*. If the smallest stable nucleus were a dimer, $E_{i*=2} \sim 1.5 \pm 0.5$ eV, in contrast with the calculated value of 0.67 eV.[35] If we instead assume that the smallest stable nucleus is a trimer, $E_{i*} = E_2 + E_3 \sim 1.5 \pm 0.6$ eV. This seems reasonable and a similar trend in formation energies was reported for the benzene molecule, which comes from the same family to that of pentacene.[39] Since $i^* = 4$ would lead to $E_{i*} \sim 1.4 \pm 0.5$ eV, which seems too low, $i^* = 3$ was most convincing estimate.

(a) 30 °C   (b) 40 °C   (c) 45 °C   (d) 50°C   (e) 60°C   (f) 75 °C   200 nm

2 μm   2 μm   2 μm   2 μm   2 μm   2 μm

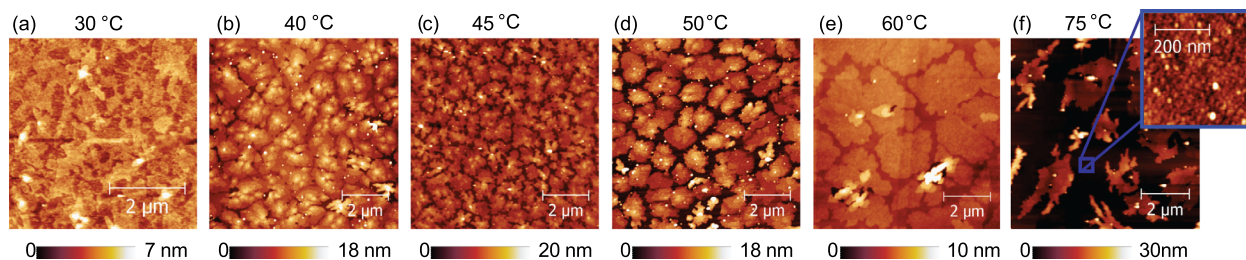0 — 7 nm   0 — 18 nm   0 — 20 nm   0 — 18 nm   0 — 10 nm   0 — 30nm

FIG. 3. 3 nm thick pentacene films deposited at substrate temperatures from 30 to 75 °C as indicated; the inset in (f) shows the interisland region with bare LSMO, $R_{rms} = 0.16$ nm, typical for LSMO.
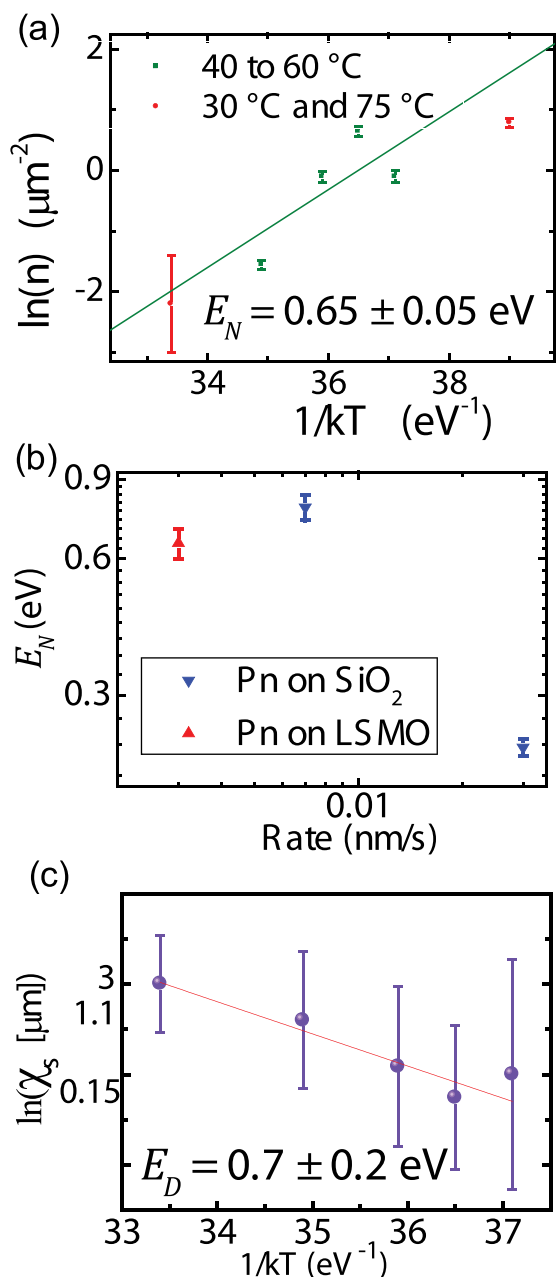
FIG. 4. (a) Islands density Arrhenius plot, from which we obtained E_N; the points from 40 °C to 60 °C are used (green square), while the red circles points are discarded because other mechanisms play a role; (b) rate dependence of E_N for pentacene (Pn) on SiO$_2$ and LSMO, data for the SiO$_2$ substrates come from literature;[35,36] (c) Arrhenius plot of the diffusion length, from which we obtained E_D.

In conclusion, we have shown that pentacene-based spin valves show spintronic effect up to room temperature.

Furthermore, we have shown that pentacene growth on LSMO is diffusion limited between 40 °C and 60 °C; we extracted the nucleation energy and the diffusion barrier, finding a weak interaction picture. When deposited at 0 °C, the surface showed lower peak to valley roughness. The observed morphology can strongly impact devices performance in ways that depend on whether the device is planar or vertical.

We firmly believe that this work not only demonstrate the feasibility of pentacene-based vertical spin valves showing that pentacene has great potential in organic spintronics applications but also maps a route towards the fabrication of improved pentacene-based spin valves.

[1]M. Pope and C. E. Swenberg, *Electronic Processes in Organic Crystals and Polymers* (Oxford University Press, 1982).
[2]V. A. Dediu, L. E. Hueso, I. Bergenti, and C. Taliani, Nat. Mater. **8**, 707 (2009).
[3]V. Dediu, M. Murgia, F. C. Matacotta, C. Taliani, and S. Barbanera, Solid State Commun. **122**, 181 (2002).
[4]M. Prezioso, A. Riminucci, I. Bergenti, P. Graziosi, D. Brunel, and V. A. Dediu, Adv. Mater. **23**, 1371 (2011); M. Prezioso, A. Riminucci, P. Graziosi, I. Bergenti, R. Rakshit, R. Cecchini, A. Vianelli, F. Borgatti, N. Haag, M. Willis, A. J. Drew, W. P. Gillin, and V. A. Dediu, *ibid.* **25**, 534 (2013).
[5]V. A. Dediu and A. Riminucci, Nat. Nanotechnol. **8**, 885 (2013).
[6]C. Wang, H. Dong, W. Hu, Y. Liu, and D. Zhu, Chem. Rev. **112**, 2208 (2012).
[7]T. W. Kelley, L. D. Boardman, T. D. Dunbar, D. V. Muyres, M. J. Pellerite, and T. P. Smith, J. Phys. Chem. B **107**, 5877 (2003).
[8]T. Ikegami, I. Kawayama, M. Tonouchi, S. Nakao, Y. Yamashita, and H. Tada, Appl. Phys. Lett. **92**, 153304 (2008).
[9]S. Toshihiro, N. Hiroyuki, N. Takuya, F. Yutaka, Y. Yukio, H. Yasushi, H. Taro, and H. Tetsuya, Jpn. J. Appl. Phys., Part 1 **47**, 1184 (2008).
[10]M. Popinciuc, Ph.D. thesis, University of Groningen, 2007.
[11]J.-Y. Hong, Y.-M. Chang, C.-H. Chuang, K.-S. Li, Y.-C. Jhang, H.-W. Shiu, C.-H. Chen, W.-C. Chiang, and M.-T. Lin, J. Phys. Chem. C **116**, 21157 (2012).
[12]I. Bergenti, V. Dediu, M. Prezioso, and A. Riminucci, Philos. Trans. R. Soc., A **369**, 3054 (2011).
[13]P. Graziosi, M. Prezioso, A. Gambardella, C. Kitts, R. K. Rakshit, A. Riminucci, I. Bergenti, F. Borgatti, C. Pernechele, M. Solzi, D. Pullini, D. Busquets-Mataix, and V. A. Dediu, Thin Solid Films **534**, 83 (2013).
[14]M. P. de Jong, V. A. Dediu, C. Taliani, and W. R. Salaneck, J. Appl. Phys. **94**, 7292 (2003).
[15]D. Nečas and P. Klapetek, Cent. Eur. J. Phys. **10**, 181 (2012).
[16]V. Dediu, L. E. Hueso, I. Bergenti, A. Riminucci, F. Borgatti, P. Graziosi, C. Newby, F. Casoli, M. P. De Jong, C. Taliani, and Y. Zhan, Phys. Rev. B **78**, 115203 (2008).
[17]T. S. Santos, J. S. Lee, P. Migdal, I. C. Lekshmi, B. Satpati, and J. S. Moodera, Phys. Rev. Lett. **98**, 016601 (2007); D. Sun, L. Yin, C. Sun, H. Guo, Z. Gai, X. G. Zhang, T. Z. Ward, Z. Cheng, and J. Shen, Phys. Rev. Lett. **104**, 236602 (2010).
[18]A. A. Sidorenko, C. Pernechele, P. Lupo, M. Ghidini, M. Solzi, R. De Renzi, I. Bergenti, P. Graziosi, V. Dediu, L. Hueso, and A. T. Hindmarch, Appl. Phys. Lett. **97**, 162509 (2010); Y. Q. Zhan, X. J. Liu, E. Carlegrim, F. H. Li, I. Bergenti, P. Graziosi, V. Dediu, and M. Fahlman, Appl. Phys. Lett. **94**, 053301 (2009).
[19]H. Chen, Z. Liu, L. Zhu, and K. Yao, "Giant Magnetoresistance Effects in the Organic spin valve La$_{0.67}$Sr$_{0.33}$MnO$_3$/Polyaniline/Co with Polyaniline as Spacer" (published online), available at http://www.paper.edu.cn/en_releasepaper/content/4506953.
[20]C. Barraud, P. Seneor, R. Mattana, S. Fusil, K. Bouzehouane, C. Deranlot, P. Graziosi, L. Hueso, I. Bergenti, V. Dediu, F. Petroff, and A. Fert, Nat. Phys. **6**, 615 (2010).
[21]J. M. De Teresa, A. Barthélémy, A. Fert, J. P. Contour, R. Lyonnet, F. Montaigne, P. Seneor, and A. Vaurès, Phys. Rev. Lett. **82**, 4288 (1999).
[22]A. C. Mayer, R. Ruiz, R. L. Headrick, A. Kazimirov, and G. G. Malliaras, Org. Electron. **5**, 257 (2004).
[23]M. G. Lagally and Z. Zhang, Nature **417**, 907 (2002).
[24]A. Al-Mahboob, Y. Fujikawa, T. Sakurai, and J. T. Sadowski, Adv. Funct. Mater. **23**, 2653 (2013).
[25]J. Krug, Physica A **340**, 647 (2004).
[26]A. Brillante, I. Bilotti, R. G. Della Valle, E. Venuti, A. Girlando, M. Masino, F. Liscio, S. Milita, C. Albonetti, P. D'Angelo, A. Shehu, and F. Biscarini, Phys. Rev. B **85**, 195308 (2012); A. C. Dürr, F. Schreiber, K. A. Ritley, V. Kruppa, J. Krug, H. Dosch, and B. Struth, Phys. Rev. Lett. **90**, 016104 (2003).

[27]F. Li, P. Graziosi, Q. Tang, Y. Zhan, X. Liu, V. Dediu, and M. Fahlman, Phys. Rev. B **81**, 205415 (2010).

[28]F. Biscarini, P. Samorí, O. Greco, and R. Zamboni, Phys. Rev. Lett. **78**, 2389 (1997).

[29]J. Villain, J. Phys. I **1**, 19 (1991).

[30]T. Toccoli, A. Pallaoro, M. Tonezzer, N. Coppedè, and S. Iannotta, Solid-State Electron. **52**, 417 (2008); Y. Wu, T. Toccoli, J. Zhang, N. Koch, E. Iacob, A. Pallaoro, S. Iannotta, and P. Rudolf, Appl. Phys. A **95**, 21 (2009).

[31]S. Pratontep, M. Brinkmann, F. Nüesch, and L. Zuppiroli, Phys. Rev. B **69**, 165201 (2004).

[32]J. A. Venables, G. D. T. Spiller, and M. Hanbucken, Rep. Prog. Phys. **47**, 399 (1984).

[33]M. Popinciuc, H. T. Jonkman, and B. J. van Wees, J. Appl. Phys. **100**, 093714 (2006).

[34]M. V. Tiba, W. J. M. de Jonge, B. Koopmans, and H. T. Jonkman, J. Appl. Phys. **100**, 093707 (2006).

[35]S. Pratontep, F. Nüesch, L. Zuppiroli, and M. Brinkmann, Phys. Rev. B **72**, 085211 (2005).

[36]M. Tejima, K. Kita, K. Kyuno, and A. Toriumi, Appl. Phys. Lett. **85**, 3746 (2004).

[37]J. G. Amar and F. Family, Phys. Rev. Lett. **74**, 2066 (1995).

[38]B. Dam and B. Stauble-Pumpin, J. Mater. Sci.: Mater. Electron. **9**, 217 (1998).

[39]H. Krause, B. Ernstberger, and H. J. Neusser, Chem. Phys. Lett. **184**, 411 (1991).